

Deuterium Nuclear Quadrupole Coupling and *cis*–*trans* Isomerization in Poly(phenylacetylene-*d*₁)

Shigeyuki Matsunami[†] and Toyoji Kakuchi^{*}

Division of Bioscience, Graduate School of Environmental Earth Science, Hokkaido University, Sapporo 060, Japan

Fumiaki Ishii

Department of Applied Physics, Faculty of Engineering, Hokkaido University, Sapporo 060, Japan

Received October 22, 1996; Revised Manuscript Received December 17, 1996[®]

ABSTRACT: Chain conformations due to thermal isomerization in poly(phenylacetylene-*d*₁) (PPA-*d*₁) were investigated by ²H solid state NMR. The observed ²H NMR line shapes at –100 °C for PPA-*d*₁ and an annealed sample, An-PPA-*d*₁, consisted of both large and small Pake doublet peaks. The former doublet peak was attributed to the static segments in the polymer chain. Deuterium nuclear quadrupole coupling constants of the large doublet peaks for PPA-*d*₁ and An-PPA-*d*₁ were 164 and 168 kHz, respectively. A quadrupole coupling constant and the formation energy of various chain conformations were calculated using semiempirical molecular orbital methods (AM1 and PM3 Hamiltonians). Agreement between theory and experiment confirmed that an exothermic peak at 177 °C in the DSC thermogram for PPA-*d*₁ is due to the *cis*–*trans* isomerization from the *cis*-transoidal form to 80°-deflected *trans*-transoidal one.

Introduction

The thermal isomerization of the polyene chain is of interest because the change from the *cis* form to the *trans* form affects molecular properties such as conductivity, second harmonic generation, and magnetism.^{1–3} All of these physical properties are closely related to the electronic states of the polyacetylene backbone. There have been many X-ray, IR, and NMR reports on the chain structure and the *cis*–*trans* isomerization of substituted polyacetylene polymerized using the various catalysts.^{4–7} In the case of NMR measurements, the thermal isomerization gave rise to an anomalous spectra in which the high-resolution ¹³C and ¹H NMR signals of the main chain become broader with the decrease of the resonance intensity.^{5,7–13} Nevertheless, it is believed that the main chain structure would be the *trans*-transoidal when the isomerization occurred, but no experimental evidence has been confirmed. In order to clarify the relationship between the broadening of the NMR spectrum and the isomerization, therefore, it is important to determine, from experiment and theory, the *cis* and *trans* forms of the main chain.

The purpose of this paper is to investigate the conformational change of the main chain of poly(phenylacetylene-*d*₁) (PPA-*d*₁) due to thermal *cis*–*trans* isomerization using the effects of deuterium nuclear quadrupole coupling on electric structures of the chain in the solid state. The exothermic isomerization and ²H NMR spectra for PPA-*d*₁ are measured as a function of temperature. The deuterium nuclear quadrupole coupling constants (NQCC's) for *cis* and *trans* forms are evaluated as a function of the deflected angle around the single bond in five conformers, using semiempirical molecular orbital approximation (AM1¹⁴ and PM3¹⁵ Hamiltonians).¹⁶ The evaluated results are compared

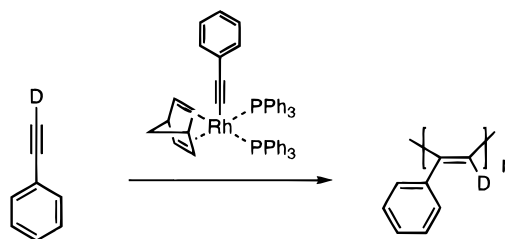


Figure 1. Polymerization of phenylacetylene-*d*₁ using Rh(C≡CC₆H₅)(nbd){Ph₃P}₂ (nbd = 2,5-norbornadiene) catalyst.

with the experimental values of NQCC in ²H NMR spectra.

Experimental Section

Samples. Phenylacetylene-*d*₁ (98% deuteriated) was purchased from Aldrich and used without purification. Polymerization of phenylacetylene-*d*₁ was carried out by using Rh(C≡CC₆H₅)(nbd){Ph₃P}₂ (nbd = 2,5-norbornadiene) catalyst reported by method of Noyori et al.¹⁷ (Figure 1).

The number-average molecular weight (*M*_n) and molecular weight distribution (*M*_w/*M*_n) of PPA-*d*₁ were *M*_n = 16 000 and *M*_w/*M*_n = 1.58, which were determined by gel permeation chromatography (GPC) using poly(styrene) as standards.

The annealed sample, An-PPA-*d*₁, was prepared in the following way: The powder sample of PPA-*d*₁ was sealed under a nitrogen atmosphere in a glass tube and annealed in an oil bath at 180 °C for 1 h. After heating, the sample was dissolved in chloroform and poured into *n*-hexane to extract the pyrolysis byproducts, 1,3,5-triphenylbenzene and oligomer.¹³ The precipitate of An-PPA-*d*₁ was filtered and dried under vacuum for 1 day. The *M*_n and *M*_w/*M*_n of An-PPA-*d*₁ were 2300 and 1.21, respectively.

NMR Measurements. Solid state ²H NMR spectra of the powder samples of PPA-*d*₁ and An-PPA-*d*₁ were measured in the temperature region between –100 and 140 °C by using a Bruker ASX-300 spectrometer operating at 46.07 MHz with the temperature-controller of Bruker B-VT2000. The standard quadrupole echo pulse sequence was 90_{±x}–τ–90_{±y}–τ–acquisition, which employed a 3.8 μs π/2 degree pulse, a delay time (τ) of 20 μs, and recycle delay of 5.0 s. The determination of the π/2 pulse width was carried out using sodium acetate-*d*₃. FIDs were acquired with 20 000 cycles, time domain size of 16 K, and spectral width of 1.25 MHz. In this case, the spectral resolution of NQCC is considered accurate to 0.076 kHz.

^{*} To whom all correspondence should be addressed. Tel: international code + 11-706-2290. Fax: international code + 11-706-7882. Email: kakuchi@e5.hines.hokudai.ac.jp.

[†] Research Fellowship of the Japan Society for the Promotion of Science.

[®] Abstract published in *Advance ACS Abstracts*, February 1, 1997.

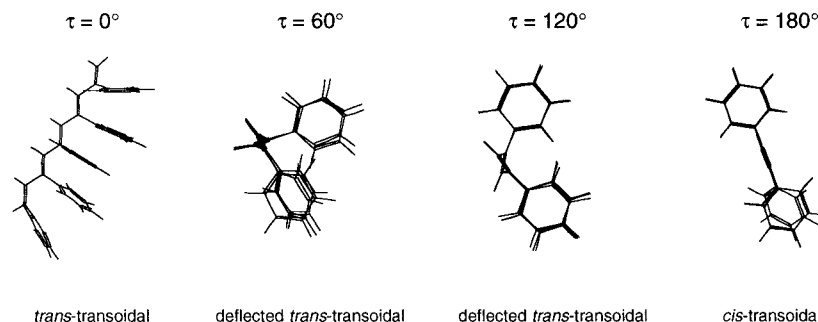


Figure 2. The back-born geometry of the deflected *trans* chain projected on the perpendicular plane to its axis. The deflected angle of τ corresponds to the dihedral angle between two double bonds in the main chain.

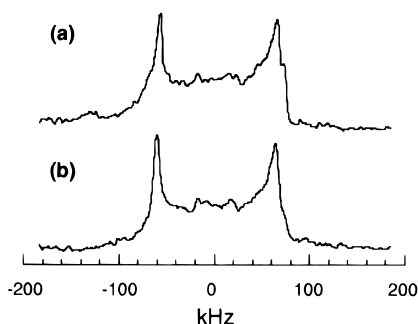


Figure 3. ^2H quadrupole echo NMR spectra of (a) PPA-*d*₁ and (b) An-PPA-*d*₁ at -100°C . The standard quadrupole echo pulse sequence was $90_{\pm x}-\tau-90_{\pm y}-\tau$ -acquisition, which employed a $3.8\ \mu\text{s}$ $\pi/2$ degree pulse, delay time (τ) of $20\ \mu\text{s}$, and a recycle delay of $5.0\ \text{s}$. FIDs were acquired with 20 000 cycles and time domain size of 16 K.

DSC and TGA Measurement. Differential scanning calorimetry (DSC) and thermogravimetric analysis (TGA) measurements were carried out in an enclosed heating chamber under flowing N_2 gas, using a Seiko Instruments SSC/5200. A heating rate of $10^\circ\text{C}/\text{min}$ was used in all experiments.

Molecular Orbital Calculations. The semiempirical molecular orbital calculations using NDDO approximation of AM1¹⁴ and PM3¹⁵ Hamiltonians were performed with the program system MOPAC version 6.0 including AnchorII software (Fujitsu) on a Fujitsu S-4/5 workstation. The geometry of the *cis* and *trans* forms for the model PPA having five conformers were built using Builder in AnchorII. In the MO calculations, we took account of not only planar zigzag structures such as *trans-transoidal*, *trans-cisoidal*, and *cis-transoidal* forms but also the same deflected conformations as TG^+TG^- -type for the *trans* chain in PVDF reported by Hasegawa et al.¹⁸

Figure 2 shows the backbone geometries of the same deflected *trans* chain conformation projected on a perpendicular plane and a perpendicular axis to its axis. The deflected angle of τ corresponds to the dihedral angle between two double bonds in the main chain. Hereafter, the dihedral angle in the deflected chain is defined as "deflected angle, τ ". The optimal geometry of various *trans* forms against the deflected angle τ was calculated in 10° intervals from $\tau = 0^\circ$ (*trans-transoidal*) to 180° (*cis-transoidal*). Formation energy of *cis-transoidal* and various deflected *trans* forms, the electron charge density on each atom, and the deuterium nuclear quadrupole coupling constant of the C-D fragment were calculated for optimal conformations in the model PPA as a function of τ .

Results

Figure 3 shows the solid state ^2H NMR spectra of PPA-*d*₁ and An-PPA-*d*₁ at -100°C , respectively. The observed ^2H NMR line shapes of each sample consist of spectra of both large and small peaks, a so-called Pake doublet powder pattern. For PPA-*d*₁ and An-PPA-*d*₁, the splitting magnitudes of the large peaks are 123 and

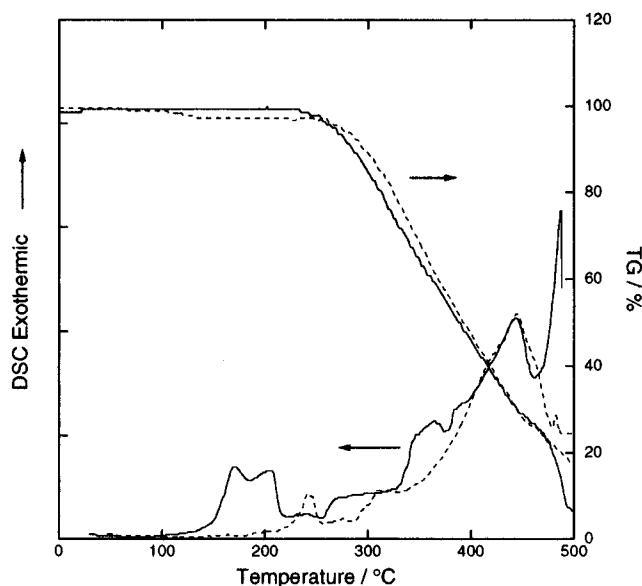


Figure 4. Differential scanning calorimetry (DSC) and thermogravimetric analysis (TGA) measurements of PPA-*d*₁ (solid line) and An-PPA-*d*₁ (dashed line) under flowing N_2 . A heating scanning rate of $10^\circ\text{C}/\text{min}$ was used in all experiments.

126 kHz, respectively, and those of the small peaks are 33 and 36 kHz. The splitting values of the large peaks for each sample did not change in the temperature region between -100 and 140°C . The asymmetry parameter of large peaks for PPA-*d*₁ and An-PPA-*d*₁ are 0.07 and 0.06, respectively.

Figure 4 shows DSC and TGA thermograms of PPA-*d*₁ and An-PPA-*d*₁ when heating at a rate of $10^\circ\text{C}/\text{min}$. An exothermic peak of PPA-*d*₁ is observed at 177 and 212°C in the DSC thermograms. In the TGA thermogram, the weight of PPA-*d*₁ decreases by 75% in the temperature region between 280 and 450°C , accompanied by a large exothermic peak at 442°C in the DSC thermogram. In the DSC thermograms of An-PPA-*d*₁, an exothermic peak is observed at 244°C . The weight of the sample decreases in the temperature region above 290°C . At 441°C , corresponding to the large exothermic peak of the DSC thermograms, the weight is 30% of the original value.

Discussion

The observed quadrupole coupling constant of deuterium in PPA-*d*₁ is obtained from the splitting magnitude of doublet peak, $\Delta\nu_q$, in the observed ^2H NMR line shape of the Pake pattern, using eq 1

$$\Delta\nu_q = \frac{3}{4} \frac{e^2 q_{zz} Q_D}{h} (3 \cos^2 \theta - 1) \quad (1)$$

In eq 1, θ is the angle that the bond vector of C–D makes with the external magnetic field, and $e^2 q_{zz} Q_D / h$ is the NQCC, where e is the charge of the electron, q_{zz} is the electric field gradient (EFG) along the C–D bond vector, and Q_D is the deuterium nuclear quadrupole moment of 2.7965×10^{-27} (cm⁻²) for deuterium ($I=1$).

The NQCC's of the C–D fragment for the large doublet peaks are 164 and 168 kHz for PPA- d_1 and An-PPA- d_1 , respectively, as calculated from the observed values of $\Delta\nu_q = 123$ and 126 kHz at $\theta = 0^\circ$ using eq 1. The NQCC values for the small doublet peaks of PPA- d_1 and An-PPA- d_1 are calculated to be 44 and 48 kHz from $\Delta\nu_q = 33$ and 36 kHz. The NQCC value for the large doublet peaks in each sample holds constant in the wide temperature region below the exothermic transition in the DSC measurement. Therefore, the NQCC of the static C–D fragments is determined to be 164 and 168 kHz from $\Delta\nu_q = 123$ and 126 kHz for PPA- d_1 and An-PPA- d_1 , respectively. The NQCC magnitude of the static C–D fragment for An-PPA- d_1 is 4 kHz larger than that of PPA- d_1 .

Let us now consider the magnitude of the NQCC values of the C–D fragment in the molecules based on the semiempirical molecular orbital methods. If the wave function ψ of a valence electron on the deuterium atom consists of a basis set of orthogonal molecular orbitals, ψ^k ($k = 1, 2, \dots, N$), the electric field gradient (EFG) of the deuterium nucleus D, q_D can be expressed as

$$q_D = -e \sum_k N^k \left\langle \psi^k \left| \frac{(3 \cos^2 \theta_k - 1)}{r_k^3} \right| \psi^k \right\rangle + e \sum_{K=1}^N \frac{Z_K (3 \cos^2 \theta_K - 1)}{r_{DK}^3} \quad (2)$$

$$= q_D^{\text{elec}} + q_D^{\text{nuc}}$$

In eq 2 the first term stands for a negative contribution from the electrons (k), where N is the number of electrons in ψ^k , and the second term is the positive contribution from the nucleus (K) to which the D atom is bonded.¹⁹ The sum is over all the other nuclei in the molecules.

In the LCAO-MO approximation, the wave function of a molecular orbital can be expressed as a superposition of atomic orbitals:

$$\psi^k = \sum_{i=1}^n c_i \phi_i \quad (3)$$

where c_i is the expansion coefficient of the i th atomic orbital function.

By substituting eq 3 into the electric term of eq 2 we get

$$q_D = \sum_k N^k \left\{ \sum_i |c_i|^2 q_D^{ii} + \sum_j |c_j|^2 q_D^{jj} + \sum_{i,j} c_i c_j q_D^{ij} + \sum_{j,k} c_j c_k q_D^{jk} \right\} + q_D^{\text{nuc}} \quad (4)$$

where

$$q_D^{\alpha\beta} = e \left\langle \phi_\alpha \left| \frac{(3 \cos^2 \theta - 1)}{r^3} \right| \phi_\beta \right\rangle \quad (\alpha, \beta = i, j, k) \quad (5)$$

and the superscript i denotes orbitals on atom D, and j

and k denote orbitals on different atoms. In eq 4, q_D^{ii} , q_D^{jj} , and q_D^{jk} are one-, and two-, and three-center integrals, respectively.

Cotton and Harris²⁰ derived the general expression of the NQCC for a given atom from eq 4 under the four simplifications of a many-center integral and the introduction of a Mulliken-type relationship on q_D^{ij} ,

$$q_D = \sum_i f_i \left\{ \bar{q}_D^{ii} + \frac{P}{\sum_i f_i} \right\} \quad (6)$$

where the bar indicates that i is summed only over noncore orbitals, and

$$f_i = \sum_K N^k |c_i|^2 + \sum_{j>i} c_i c_j S_{ij} \quad (7)$$

where S_{ij} is the overlap integral. The expression for f_i in eq 7 can be given a simple physical interpretation in terms of the electron density on the deuterium atom and the bond order of the C–D bond, which comes from the sp^2 hybridization orbital of carbon in the C–D bond. In eq 6, $P/\sum_i f_i$ is the polarization term of the sum over all core orbitals, i.e., the Sternheimer correction. If the values of the polarization term may be neglected, then the NQCC is rewritten to be

$$\frac{eq_D Q_D}{h} = \sum_i f_i \left\{ \frac{e \bar{q}_D^{ii} Q_D}{h} \right\} \quad (8)$$

Therefore, from eq 2 to 8, the deuterium NQCC would be sensitive to the electric structure of the double bond and the C–D bond length for the chain conformation, unless the nuclear field gradient of the carbon in the C–D bond is overwhelmingly predominant in the EFG of deuterated PPA samples.

To clarify the relationship between the chain conformations and the NQCC values, the electron density, the C–D bond order, and C–D bond length were calculated using the NDDO approximation of AM1 and PM3 for the five conformers of PPA. In addition, we also calculated the heat of formation, ΔH_f to evaluate the stability of the chain conformations. In the MO calculations, we took account of not only planar zigzag forms such as *trans-transoidal*, *trans-cisoidal*, and *cis-transoidal* forms, but also the same deflected conformations as TG⁺TG⁻-type for the *trans* chain in PVDF reported by Hasegawa et al.¹⁸ The optimal geometries of various conformations against the deflected angle τ were calculated in 10° intervals from $\tau = 0^\circ$ (*trans-transoidal*) to 180° (*cis-transoidal*) as described in Figure 2.

Figure 5 shows the deflected angle dependence of the ΔH_f for various conformations. The calculated energies of ΔH_f values for *trans-cisoidal* (tc), *cis-transoidal* (ct), and *trans-transoidal* (tt) forms become larger in the order $\Delta H_f^{\text{tc}} < \Delta H_f^{\text{ct}} < \Delta H_f^{\text{tt}}$, as listed in Table 1.

The order of the ΔH_f was similar with the results of TC-1, CT-1, and T-2 head-to-tail isomers for the six-conformers of PPA which were obtained by Matsuzawa and Dixon.²¹ The minimum ΔH_f value is 219.19 kcal/mol at $\tau = 130^\circ$, as calculated using AM1. Furthermore, ΔH_f remains constant at 222.00 kcal/mol in the range of $\tau = 90^\circ$ – 80° . In contrast, in the PM3 calculation, the ΔH_f curve shows only one minimum value of 211.23 kcal/mol at $\tau = 100^\circ$.

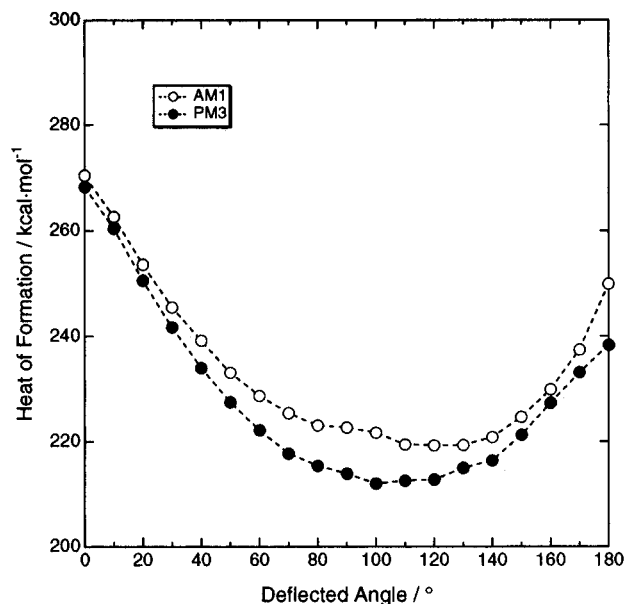


Figure 5. Deflected angle dependence of the heat of formation energy in PPA of five conformers using AM1 and PM3 Hamiltonians. The deflected angle of τ corresponds to the dihedral angle between two double bonds in the main chain. The optimal geometry of various *trans* forms against the deflected angle was calculated at an interval of 10° .

Table 1. Heat of Formation (ΔH_f) of *cis*-Transoidal, *trans*-Cisoidal, and *trans*-Transoidal Forms for PPA Using AM1 and PM3 Hamiltonians

	ΔH_f (kcal/mol)		
	<i>cis</i> -transoidal	<i>trans</i> -cisoidal	<i>trans</i> -transoidal
AM1	249.95	242.19	270.45
PM3	238.31	235.53	268.34

Table 2. Minimum Heat of Formation (ΔH_f^{\min}) and Its Deflected Angle (τ_{\min}) for PPA Using AM1 and PM3 Hamiltonians

AM1		PM3	
τ_{\min} (deg)	ΔH_f^{\min} (kcal/mol)	τ_{\min} (deg)	ΔH_f^{\min} (kcal/mol)
80	222.0	100	211.23
140	219.19		

Table 2 summarizes the values of the minimum ΔH_f^{\min} values and the corresponding angles τ_{\min} in AM1 and PM3 calculations. Although there is a slight difference of τ_{\min} on ΔH_f^{\min} between AM1 and PM3, the minimization of each ΔH_f vs τ curve indicates that the deflected *trans* chain conformation is more stable than the *cis*-transoidal, *trans*-cisoidal, and *trans*-transoidal forms.

Using the observed value of $eq_D Q_D/h = 164$ kHz for PPA-*d*₁ and the calculated values of f_i (AM1) = 1.7413 and f_i (PM3) = 1.7539 in eq 8, we obtained NQCC of the free deuteron, $e^2 q_D^2 Q_D/h$, as 93.5 kHz (AM1) and 92.9 kHz (PM3), assuming a *cis*-transoidal form of PPA-*d*₁.¹⁷ The theoretical values of NQCC at the deflected angle of τ for the *trans*-transoidal conformations in the AM1 and PM3 calculations are corrected using the respective NQCC values of the *cis*-transoidal conformers.

Figure 6 shows the deflected angle dependencies on NQCC values and on C–D bond length. The τ dependence on C–D bond length was the same for both AM1 and PM3 calculations. As the deflected angle τ decreases away from the *cis*-transoidal form, the C–D bond length of the chain form decreases and becomes constant at 1.095 Å below $\tau = 90^\circ$. On the other hand,

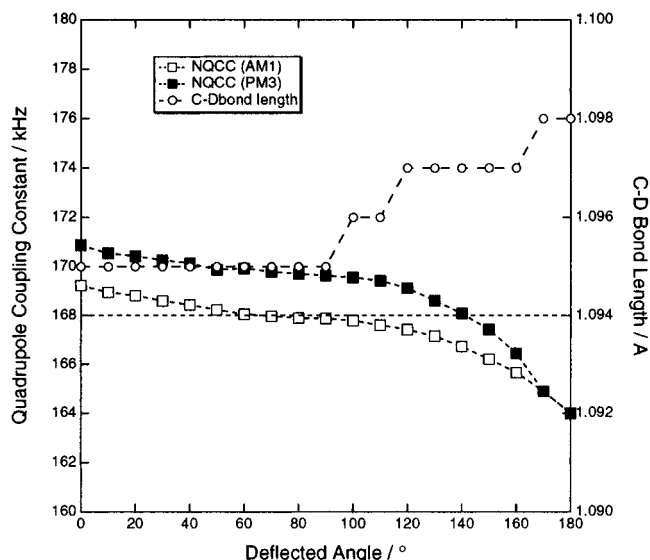


Figure 6. Deflected angle dependencies of the nuclear quadrupole coupling constant (NQCC) and C–D bond length in PPA of five conformers using AM1 and PM3 Hamiltonians. The NQCC of the free deuteron, $e^2 q_D^2 Q_D/h$ due to the sp^2 hybrid orbital in eq 8 is estimated to be 93.5 and 92.9 kHz for AM1 and PM3, respectively, from the observed value of $e^2 q_D^2 Q_D/h = 164$ kHz for PPA-*d*₁ and the calculated values of f_i (AM1) = 1.7413 and f_i (PM3) = 1.7539.

the NQCC increases rapidly between $\tau = 180^\circ$ and 90° , and gradually from $\tau = 90^\circ$ to 0° with the decrease of τ . All the values of NQCC in the PM3 calculation are larger than those of AM1 in the whole τ region. Olympia et al. reported that the deuterium NQCC value of the C–D fragment for the C–C bonds of the sp , sp^2 , and sp^3 orbitals in molecules increases with the decrease of the C–D bond length.²² These findings indicate that this change of C–D bond length on the deflected angle τ depends strongly on the electric state of sp^2 orbital in the C=C bond when the τ changes about the single bond of C–C.

Here, we will estimate the main chain conformation as a result of annealing the polymer, in term of the deflected angle τ determined by analysis of the NQCC value. The dotted line in Figure 6 is the experimental NQCC value of 168 kHz. This experimental value corresponds to the theoretical value when $\tau = 80^\circ$, as determined with AM1, and to $\tau = 140^\circ$, using PM3. The formation energy of the deflected *trans*-transoidal form is $\Delta H_f = 222$ kcal/mol for AM1 (i.e. $\tau = 80^\circ$) and $\Delta H_f = 215$ kcal/mol for PM3 (i.e. $\tau = 140^\circ$); see Figure 5. The AM1 ΔH_f value is 28 kcal/mol smaller than the ΔH_f of the *cis*-transoidal form ($\tau = 180^\circ$) and 3 kcal/mol larger than the ΔH_f^{\min} . The PM3 ΔH_f value is 23 kcal/mol smaller than the ΔH_f of the *cis*-transoidal form and 4 kcal/mol larger than the ΔH_f^{\min} . Since the difference between the ΔH_f corresponding to the experimental NQCC and ΔH_f^{\min} in AM1 is 1 kcal/mol smaller than that in PM3, the 80° -deflected *trans*-transoidal form is considered a more stable structure than the 140° -deflected one. Therefore, the 4 kHz difference between PPA-*d*₁ and An-PPA-*d*₁ NQCC values is attributed to the difference of main chain structure between *cis*-transoidal ($\tau = 180^\circ$) for PPA-*d*₁ and 80° -deflected *trans*-transoidal for An-PPA-*d*₁.

In contrast to PPA-*d*₁, no exothermic peak for An-PPA-*d*₁ is observed in the DSC thermogram below 230°C , as shown in Figure 4. It is confirmed from such NMR and DSC results that the exothermic peak of DSC

thermograms at 177 °C for PPA-*d*₁ is attributed to the *cis*–*trans* isomerization from the *cis*-transoidal form to the deflected *trans*-transoidal one, as well as the solid state ¹H NMR analysis of *cis*–*trans* isomerization on the DSC exothermic peak at 180 °C for crowned PPA.²³ We also reported that *cis*–*trans* isomerization of PPA accompanied the formation of 1,3,5-triphenylbenzene and the decrease of molecular weight at the DSC exothermic temperature.¹³ The exothermic peak observed at 212 °C in the PPA-*d*₁ DSC thermograms, as well as that at 244 °C for An-PPA-*d*₁, may be attributed to the hydrogen migration accompanying a cross-linking reaction, i.e., the formation of triphenylbenzenes from the deflected *trans* chains. The 32 °C higher temperature shift for this peak in An-PPA-*d*₁ suggests that the deflected *trans* chains in the solid state are more thermostable. The larger exothermic peak above 300 °C accompanies the large weight loss in the TGA thermograms for each sample, which may be attributed to the cross-linking reaction with the thermal decomposition, in contrast to the endothermic phenomena of poly(acetylene).²⁴

²H NMR analyses of the anomalous ²H NMR line shape of the C–D fragments in the chain end segment for PPA-*d*₁ and the phenyl groups for PPA-*d*₅ will be reported in more detail elsewhere in the near future.

Conclusions

The solid state ²H NMR spectra of poly(phenylacetylene-*d*₁), PPA-*d*₁, and its annealed sample, An-PPA-*d*₁, were measured at –100 °C. The observed ²H NMR spectra for each sample consisted of both large and small doublet peaks. Since the 164 and 168 kHz quadrupole coupling constants of the large peaks for PPA-*d*₁ and An-PPA-*d*₁ were insensitive to a change in temperature, the large doublet peaks are attributed to static main segments in the polymer chain.

The optimal geometry, the deuterium nuclear quadrupole coupling constants, and the formation energies of various chain conformations were calculated using both AM1 and PM3 semiempirical molecular orbital methods as a function of the deflected angle τ from $\tau = 0^\circ$ (*trans*-transoidal) to 180° (*cis*-transoidal). The chain conformation of An-PPA-*d*₁ was determined to be a 80°-deflected *trans*-transoidal form in AM1, which is more thermostable than the *cis*-transoidal form of PPA-*d*₁. This determination of the chain conformation confirmed that an exothermic peak at 177 °C in the DSC thermo-

gram for PPA-*d*₁ is due to the *cis*–*trans* isomerization from the *cis*-transoidal form to the 80°-deflected *trans*-transoidal one.

Acknowledgment. This work was supported by the Research Fellowship of the Japan Society for the Promotion of Science for Young Scientists.

References and Notes

- (1) Chien, J. C. W. *Polyacetylene: Chemistry, Physics, and Material Science*; Academic: Orlando, FL, 1984.
- (2) Fujii, A.; Ishida, T.; Koga, N.; Iwamura, H. *Macromolecules* **1991**, *24*, 1077.
- (3) Miura, Y.; Matsumoto, M.; Ushiotani, Y.; Teki, Y.; Takui, T.; Itoh, K. *Macromolecules* **1993**, *26*, 6673.
- (4) Berlin, A. A.; Cherkashin, M. I.; Chernysheva, I. P.; Aseyev, Y. G.; Barkan, Y. I.; Kisilitsa, P. P. *Vysokomo. soyed.* **1967**, *9*, 1840.
- (5) Simionescu, C. I.; Percec, V.; Dumitrescu, S. *J. Polym. Sci., Polym. Chem. Ed.* **1977**, *15*, 2497.
- (6) Simionescu, C. I.; Percec, V. *J. Polym. Sci., Polym. Chem. Ed.* **1980**, *18*, 147.
- (7) Furlani, A.; Licoccia, S.; Russo, M. V.; Camus, A.; Marsich, N. *J. Polym. Sci., Part A, Polym. Chem.* **1986**, *24*, 991.
- (8) Berlin, A. A.; Cherkashin, M. I. *Vysokomol. Soyed.* **1971**, *10*, 2298.
- (9) Simionescu, C. I.; Percec, V. *J. Polym. Sci. Polym. Lett. Ed.* **1979**, *17*, 421.
- (10) Sanford, T. J.; Allendoerfer, R. D.; Kang, E. T.; Ehrlich, P. *J. Polym. Sci., Polym. Phys. Ed.* **1980**, *18*, 2277.
- (11) Lee, D.-H.; Lee, D.-H.; Soga, K. *Macromol. Rapid Commun.* **1990**, *11*, 559.
- (12) Kakuchi, T.; Matsunami, S.; Kamimura, H.; Ishii, F. *J. Polym. Sci., Part B, Polym. Phys.* **1995**, *33*, 2151.
- (13) Matsunami, S.; Watanabe, T.; Kamimura, H.; Ishii, F.; Tsuda, K.; Kakuchi, T. *Polymer*, **1996**, *37*, 4853.
- (14) Dewar, M. J. S.; Zebisch, E. G.; Healy, E. F.; Stewart, J. J. P. *J. Am. Chem. Soc.* **1985**, *107*, 3902.
- (15) Stewart, J. J. P. *J. Comput. Chem.* **1989**, *10*, 209.
- (16) Jackisch, M. A.; Jarrett, W. L.; Guo, K.; Fronczek, F. R.; Butler, L. G. *J. Am. Chem. Soc.* **1988**, *110*, 343.
- (17) Kishimoto, Y.; Eckerle, P.; Miyatake, T.; Ikariya, T.; Noyori, R. *J. Am. Chem. Soc.* **1994**, *116*, 12131.
- (18) Hasegawa, R.; Kobayashi, M.; Tadokoro, H. *Polymer J.* **1972**, *3*, 591.
- (19) Caves, T.; Karplus, M. *J. Chem. Phys.* **1966**, *45*, 1670.
- (20) Cotton, F. A.; Harris, C. B. *Proc. Natl. Acad. Sci. U.S.A.* **1966**, *56*, 12.
- (21) Matsuzawa, N.; Dixon, D. A. *J. Phys. Chem.* **1994**, *98*, 11669.
- (22) Olympia, P. L.; Wei, I. Y.; Fung, B. M. *J. Chem. Phys.* **1969**, *51*, 1610.
- (23) Matsunami, S.; Kakuchi, T.; Ishii, F. *submitted to J. Polym. Sci., Polym. Phys. Ed.*
- (24) Ito, T.; Shirakawa, H.; Ikeda, S. *J. Polym. Sci., Polym. Chem. Ed.* **1975**, *13*, 1943.

MA9615664